Design of a high-performance centrifugal compressor with new surge margin improvement technique for high speed turbomachinery

Pakle, Sagar; Jiang, Kyle

DOI:
10.1016/j.jppr.2018.02.004

Document Version
Publisher's PDF, also known as Version of record

Citation for published version (Harvard):
Pakle, S & Jiang, K 2018, 'Design of a high-performance centrifugal compressor with new surge margin improvement technique for high speed turbomachinery', *Propulsion and Power Research*, vol. 7, no. 1, pp. 19-29. https://doi.org/10.1016/j.jppr.2018.02.004

Published in Propulsion and Power Research
https://doi.org/10.1016/j.jppr.2018.02.004

Propulsion and Power Research 2018;7(1):19–29

HOSTED BY

ELSEVIER

http://ppr.buaa.edu.cn/

Propulsion and Power Research

www.sciencedirect.com

ORIGINAL ARTICLE

Design of a high-performance centrifugal compressor with new surge margin improvement technique for high speed turbomachinery

Sagar Pakle, Kyle Jiang*

School of Engineering, University of Birmingham, Edgbaston, Birmingham B15 2TT, United Kingdom

Received 17 February 2017; accepted 14 December 2017
Available online 15 March 2018

KEYWORDS

Centrifugal compressor;
Aerodynamic performance;
Surge margin;
Blade angles;
Stress analysis;
Computational fluid dynamics

Abstract This paper presents the design of a centrifugal compressor for high-speed turbomachinery. The main focus of the research is to develop a centrifugal compressor with improved aerodynamic performance. As a meridional frame has a significant effect on overall performance of the compressor, special attention has been paid to the end wall contours. The shroud profile is design with bezier curve and hub profile with circular arc contour. The blade angle distribution has been arranged in a manner that it merges with single value at impeller exit. The rake angle is positive at leading edge and negative at trailing edge with identical magnitude. Furthermore, three-dimensional straight line element approach has been used for this design for better manufacturability. The verification of the aerodynamic performance has been carried out using CFD software with consideration of a single blade passage and vaneless diffuser. The result has been compared with matching size aftermarket compressor stage gas stand data. The compressor stage with Trim 55 provides 34% increase in choke flow at 210000 RPM as compared to gas stand data with 87% peak stage efficiency at 110000 RPM. In addition, new surge margin improvement technique has been proposed by means of diffuser enhancement. This technique provides an average of 16% improvement in surge margin compared to standard diffuser stage with 55 trim compressor impeller. The mechanical integrity has been validated at maximum RPM with the aluminum alloy 2014-T6 as a fabrication material.

*Corresponding author. Tel.: +44 (0) 121 414 6800.
E-mail address: k.jiang@bham.ac.uk (Kyle Jiang).

Peer review under responsibility of National Laboratory for Aeronautics and Astronautics, China.

https://doi.org/10.1016/j.jppr.2018.02.004

Nomenclature

I	total work factor/work input coefficient
H	enthalpy (unit: J)
U	blade tip speed (unit: m/s)
B	fractional aerodynamics area blockage, hub to shroud passage width (unit: mm)
$\overline{\omega}$	total pressure loss coefficient
Pv	velocity pressure, P_0-P (unit: Pa)
Z	number of blades
P	pressure (unit: Pa)
d	diameter (unit: mm)
L	length of mean camber line (unit: mm)
η	efficiency
C_p	static pressure recovery coefficient

Greek letters

α	angle between streamline slop with axial direction
λ	impeller tip distortion factor
σ	slip factor
δ	clearance gap parameter

Subscripts

B	blade
c	compressor
D	diffuser
SF	skin friction
v	velocity
H	hydraulic
CL	clearance
1	impeller blade inlet condition
2	impeller blade outlet condition
3	diffuser outlet condition

1. Introduction

The development of high-performance centrifugal compressor for the application of high-speed turbomachinery such as turbochargers and micro gas turbines needs to be addressed urgently due to the fact that it offers enormous opportunities to control the exhaust emission in automobile engines and makes it more environmentally friendly. Specifically, the development of high-performance turbochargers for automobile engines are attracting more attention since it has a direct impact on the engine power, specific fuel consumption and exhaust emission level. As global emission authorities are issuing strict guidelines for exhaust emission levels, it is necessary for the automotive industry to alleviate an emission rate to comply with the global emission standard. This could be achieved by incorporating turbochargers into automobile engines, which essentially increases the mean effective pressure (the ratio of torque to the volume of the engine) and enhance engine performance. In addition to that, this target can be more efficiently achieved by designing a centrifugal compressor for turbochargers with enhanced performance and additional distinct qualities as lower wheel inertia to promote a rapid acceleration and better transient response of compressor during the course of engine operation [1]. Moreover, as an application of centrifugal compressor is found in various domains such as aerospace, automotive industry, oil and gas industry, and power generation, the demand for improving performance is enormous, particularly in terms of compressor efficiency and mass flow range [2].

Interestingly, development in a centrifugal compressor is more appealing to turbocharger industry due to the fact that existing compressor wheels are unable to meet the required performance target in terms of efficiency and flow range. Currently, passenger vehicle turbochargers provide 75% to 78% peak stage efficiency with wheel peak efficiency around 82% to 84%, considering the fact that most of the total pressure loss takes place in diffuser and volute and significantly affect overall stage efficiency. Therefore, in this scenario, increase in stage efficiency and compressor map flow range is highly demanded. Nevertheless, development of a diesel engine is rapidly being done to meet the emission standard; therefore, compatible turbocharger with better flow range and efficiency is essentially anticipated. This fact promotes the development of improved performance compressor wheel with lower inertia which subsequently results in better transient response.

The proposed centrifugal compressor design is targeted for turbochargers applicable to 1.6 - 2 liter diesel engines with an intent of providing a required boost pressure, wide flow range, and improved peak efficiency. The design has been accomplished by firstly designing the meridional frame and subsequently converting it into a three-dimensional design with three-dimensional straight line elements. An approach proposed by Aungier [3] has been implemented for preliminary design. Through this approach distribution of hub and shroud blade angles has been devised. However, special attention has been given for hub blade angle since it has significant effect on wheel efficiency [4]. Likewise, impeller key dimensions such as an exducer b-width, an inducer diameter, and flow angles have been established through correlation proposed by Aungier [3]. Meanwhile, some of the design constraints have been imposed in terms of fixed values in order to take account of compactness of impeller.

Apart from that, greater challenge lies in concluding on compressor exducer maximum tip speed and back sweep angle due to structural limitations. In order to achieve the required pressure ratio, back sweep angle needs to be minimized which penalize the flow range. Work input

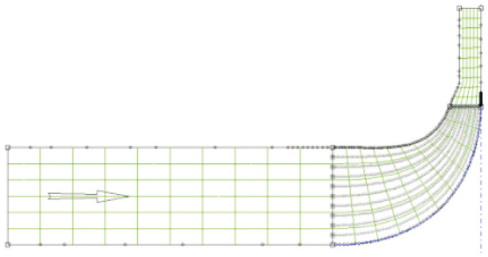

Figure 1 The meridional plot for a centrifugal compressor.

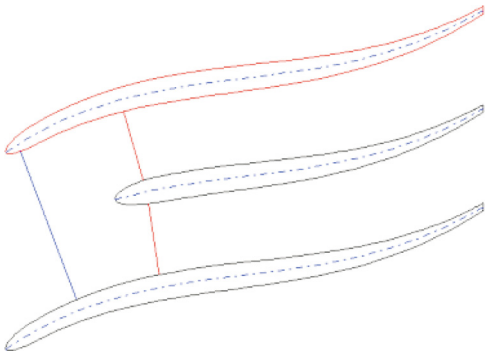

Figure 2 Blade-to-blade view.

coefficient $I = \Delta H/U^2$ is another parameter which controls the tip speed. Higher blade angle (lower swirl velocity) and flow coefficient reduce the work coefficient [5]. Therefore, optimizing work coefficient and trade off among total pressure ratio, flow range and back sweep angle play a vital role in overall performance of centrifugal compressor with structural integrity.

2. Preliminary design

A preliminary design of the compressor has been carried out with a tip speed of 427 m/s having 44 mm exducer diameter. The flow coefficient of 0.18, polytropic efficiency 92% and total pressure ratio 2.5 has been taken as design point attributes.

As the properties of the flow have a significant effect on the compressor performance, care must be taken while defining the accurate fluid properties [6]. In this preliminary design, a thermally perfect gas model for air with a molecular weight of 28.96 g/mol has been considered. In addition to that, aerodynamics losses such as tip clearance loss, friction loss, and recirculation loss have been accounted in calculations which have substantial impact on overall performance of the stage [3]; in fact, it is essential to take account of loss correlation into preliminary design calculation to fetch an accurate estimation of performance target.

Taking account of all above facts, a quick estimate of geometric parameters and performance data can be obtained under the given design conditions. Hence, this method facilitates the quick insight into the possible extent of performance which can be achieved through obtained design configuration and provide an estimation of velocity triangle at inlet and outlet of the compressor in an absolute and relative frame of reference. It is worth noting that the compressor meridional profile has a significant effect on the total pressure ratio and efficiency, therefore, it is essential to design a meridional plot with proper attention [7]. In a context of present design, the meridional sketch has been designed at a preliminary stage with the help of bezier shroud curve and circular arc hub contour. The shroud curve has been further adjusted to make it streamlined. The final meridional plot with diffuser sketch is shown in Figure 1.

3. The inlet of impeller

The inlet of impeller has a substantial influence on the overall performance of the compressor. An inlet diameter or the square of the inlet to outlet diameter ratio (trim) has a significant effect on the maximum flow capacity of compressor [1]. Moreover, the magnitude of inlet diameter is governed by inlet relative flow angle. Therefore, to achieve a required flow capacity it is necessary to tune inlet relative flow angle accordingly. In the present design, to achieve inlet shroud diameter of 34.08 mm (Trim 60) with hub diameter of 13 mm, the magnitude of inlet relative flow angle is set to be 34.58°. Furthermore, due to high trim and high mass flow, inlet relative Mach number at compressor inducer approaches to supersonic value which results in shock waves, which subsequently casues shock losses and should be kept within a limit. Therefore, precautions must be exercised to optimize inducer diameter in order to keep relative Mach number as minimum as possible.

4. Impeller outlet

The performance of centrifugal compressor is largely influenced by blade exducer, blade outlet angle, and outlet diameter. Although an exit diameter of 44 mm has been set based on the designer's decision, the b-width of the blade and the outlet angle need to be optimized to achieve required aerodynamic performance, as these parameters have a substantial effect on mass flow capacity, total pressure ratio and adiabatic efficiency [7]. Furthermore, tip flow angle governs b-width of the exducer and it is recommended to keep the tip flow angle from 60° to 75° [5]. However, with the given design conditions and in order to keep relative velocity ratio w_2/w_1 in a range from 0.70 to 0.95, a tip flow angle has been set to 40° which results in relative velocity ratio of 0.91 and exducer b-width of 3.26 mm.

Likewise, the tip blade angle β_2 has a dominant effect on flow range and adiabatic efficiency and happens to be the most import variable in stress perspective which influences

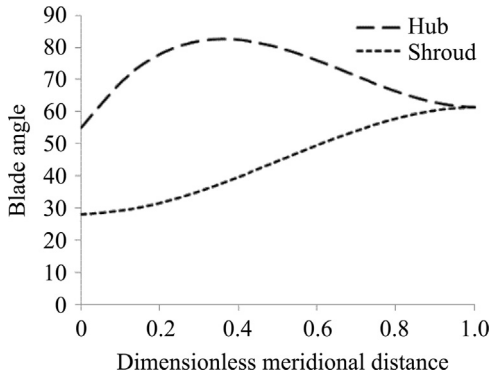

Figure 3 Blade angle distribution.

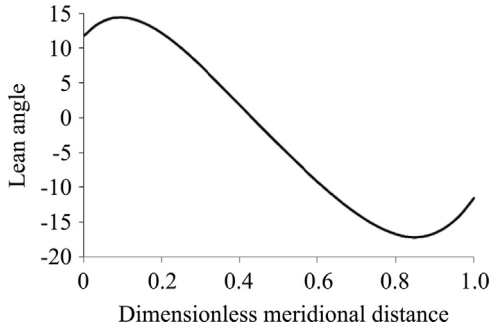

Figure 4 Lean angle distribution.

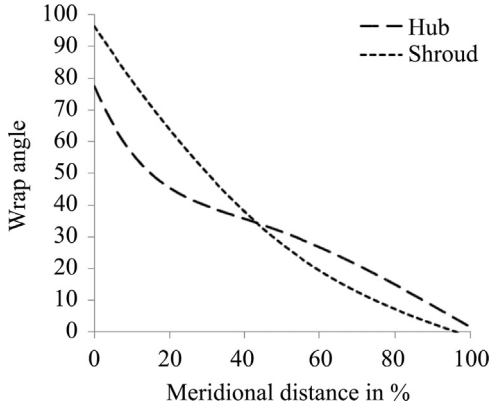

Figure 5 Wrap angle distribution.

the stress intensity at blade exducer. Essentially, tip blade angle is based on the slip factor σ and impeller blade work input I_B and can be achieved iteratively through following equations suggested by Aungier [3].

$$\sigma = 1 - \sqrt{\sin\beta_2}\,\frac{\sin\alpha_{c2}}{Z^{0.7}} \tag{1}$$

$$I_B = \sigma\left(1 - \lambda C_{m2}\,\frac{\cot\beta_2}{U_2}\right) \tag{2}$$

where, impeller tip distortion factor λ and impeller work input I_B given as

$$\lambda = \frac{1}{1 - B_2} \tag{3}$$

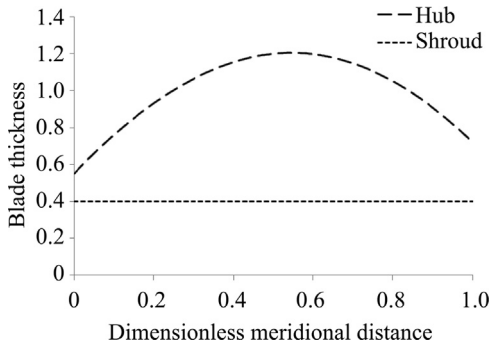

Figure 6 Blade thickness distribution.

$$I_B = \frac{C_{u2}}{U_2} \tag{4}$$

In this case, B_2 is a tip fractional are blockage can be estimated as:

$$B_2 = \overline{\omega}_{SF}\,\frac{P_{v1}}{P_{v2}}\sqrt{\frac{W_1 d_H}{W_2 b_2}} + \left[0.3 + \frac{b_2^2}{L_B^2}\right]\frac{A_R^2 \rho_2 b_2}{\rho_1 L_B} + \frac{\delta_{CL}}{2b_2} \tag{5}$$

where A_R is a ratio of the impeller tip flow area to the throat area and defined by

$$A_R = \frac{A_2 \sin\beta_2}{A_1 \sin\beta_{th}} \tag{6}$$

and β_{th} is a blade suction surface angle at throat.

5. Detailed impeller design

Three-dimensional straight line elements have been used to generate three-dimensional impeller design with constant axial dimension inlet and constant radial dimension outlet. Splitter blades are employed at half pitch location to maximize the flow and to decrease the blade loading on full blades. The geometry of splitter blade is the same as the full blade which starts at 15% of hub meridional length and ends at the same location as full blade end with cut-off trailing edge. The blade-to-blade view of blades is shown in Figure 2.

Blade angle distribution makes significant contribution to the performance of compressor therefore an accurate approach needs to be taken to devise a blade angle along camber line for better aerodynamics performance. In the design, the distribution of blade angle for the shroud and hub camber line is done with correlation proposed by Aungier [3]. In this case, the values of the blade angle at leading edge differ for hub and shroud. However, along the meridional distance, the blade angle converges towards the trailing edge. In this method, precaution is taken to set the gradient of blade angle to zero at trailing edge to minimize the uncertainty in a work input prediction and at blade inducer to minimize the blade loading at high Mach number [3]. The blade angle distribution measured with respect to tangential direction is shown in Figure 3.

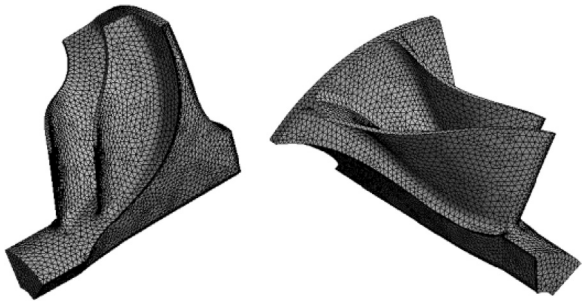

Figure 7 Unstructured finite element mesh.

In line with that, rake or lean angle positively affects the exit flow behavior and adiabatic efficiency. In general, a blade lean can contribute to performance by means of improving peak efficiency and widening operation range [8]. In the current design, 11.60° rake angle at leading edge and - 11.60° rake angle at trailing edge is used as shown in Figure 4.

In addition, skin friction on the blade surface is proportional to a camber of the blade [9]. Therefore, the camber of the blade needs to be minimized which can be accomplished by reducing the blade wrap angle at hub and shroud region. The distribution of wrap angle along the meridional distance for this design, shown in Figure 5, illustrates that the magnitude of the wrap angle steadily decrease from leading edge to zero at the trailing edge of the blade.

Furthermore, in the context of structural integrity of compressor blade, it is essential to provide a suitable thickness of blade such that it can withstand the high centrifugal stress during operation at high speeds. In the current design where six main and splitter blades are present, the shroud has constant thickness whereas the thickness of hub varies from leading edge to trailing edge. The distribution of blade thickness is shown in Figure 6. In addition, in order to minimize the boundary layer losses and improve aerodynamic performance, the leading edge of blades is modeled with an elliptical ratio of 4:1 at hub and 6:1 at shroud whereas the trailing edge is kept cut off.

6. Structural integrity

Integration of finite element analysis into the design process to validate the structural strength of the design is of paramount importance. This is due to the fact that the compressor wheel experiences severe loading during its operation and its ability to withstand these loads need to be evaluated for the successful operation. These loads are mainly caused by centrifugal force, vibration and aerodynamic forces on the blade. Therefore it is imperative to validate mechanical strength of the compressor wheel to avoid catastrophic damage. In the present design, an assessment of mechanical integrity has been carried out using a sector of an impeller. The material used for this assessment is aluminum alloy 2014-T6 which has a minimum yield strength of 345 kPa with material density of

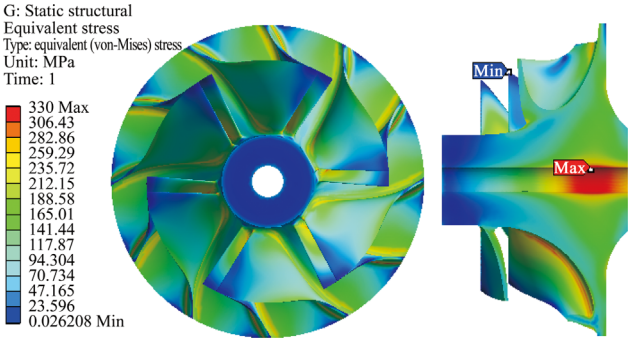

Figure 8 Equivalent (von-mises) stress.

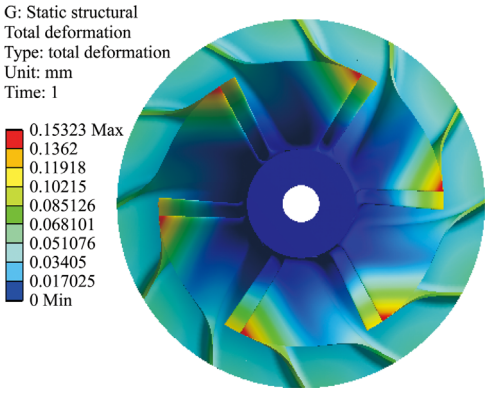

Figure 9 Total deformation.

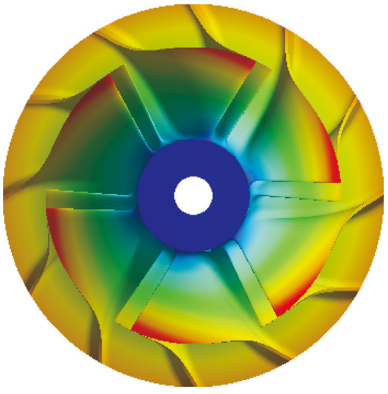

Figure 10 1st mode at blade inducer (modal analysis).

2780 kg/m^3. This sector consists of one main and one splitter blade with back disk outer diameter thickness of 1 mm. This sector geometry has been meshed with unstructured finite elements as shown in Figure 7.

It is necessary to validate the strength of a blade when it is subject to severe centrifugal loading. Since the intensity of the loading is proportional to rotational speed, stress validation has been carried out at maximum speed of 230,000 RPM. In the validation process, static structural strength analyzed followed by modal analysis to quantify the magnitude of blade frequency. For this analysis fixed constraint boundary condition at hub was applied. The result shows a maximum stress appears in the bore with a

magnitude of 330 MPa which is well below the yield strength of 345 MPa for the aluminum alloy. Furthermore, exducer hub and leading edge root region are other locations where higher stress are observed, but their magnitudes are well below the maximum value in the bore. The contours of stress distribution are shown in Figure 8.

As the compressor wheel is subject to the centrifugal stress, it undergoes a certain level of deformation. The magnitude and locations of the deformation are important both to the design and to its operation since it can cause contact with the compressor housing and also adversely influence aerodynamic efficiency of the compressor. In the analysis, the maximum deformation of 0.153 mm is observed at inducer region as shown in Figure 9, which can be considered as acceptable, as it would not make any significant change in aerodynamic performance of the wheel and clearance between the blades and housing can be designed accordingly.

Furthermore, it is necessary to cross check the running frequency of a single blade and compare it with the resinate frequency of it to avoid overlap. An assessment of blade frequency has been carried out through modal analysis with inclusion of pre-stress effect from the static structural solution. The result obtained shows that the first frequency is more than 4 times higher than the natural frequency of the blade and the first frequency mode shape occurs at main blade inducer region which is shown in Figure 10.

7. Computational fluid dynamics

Prediction of aerodynamic performance of a compressor accurately plays a vital role in the design process. Every design needs to be validated by viscous flow calculations which provide performance estimate with viscous losses. Although experimental techniques are best suited to validate the performance, the cost and time of applying the technique could be unaffordable for design iterations. Nowadays, computational fluid dynamics (CFD) has become a cost effective tool to provide a predictions of performance with acceptable accuracy.

In the present design, CFD simulations have been carried out using finite volume based package ANSYS-CFX. Prior to this analysis, a grid independence study for slightly higher diameter wheel was carried out with domain grid size varying from 0.5 million to 2.0 million nodes in order to standardize the grid size. The details of the grid size and its influence on the stage performance parameters are shown in Table 1.

Hence, based on this grid independence study, the mesh with approximately one million of nodes has been accepted while keeping first element height of 5e-6 m in order to get $y+$ value from 1 to 5. The resultant mesh is shown in Figure 11.

In addition, near wall turbulence plays an important role in the outcome of aerodynamic performance, hence it is essential to add turbulence model with the capability to model near wall turbulence to CFD simulations. In the current case, Shear stress transport (k-ω SST) turbulence model has been implemented which is proven to be better for rotating flows [4]. In the context of geometrical configuration, CFD simulation was carried out with stage comprising a single blade passage and vaneless diffuser. A diffuser width devised to be 2.4 mm at diffuser outlet and location of diffuser exit is set to be 1.5 times the blade trailing edge. The outline of compressor stage is shown in Figure 12.

A qualitative performance of flow obtained through CFD simulations has significant importance since it describes the behavior of flow throughout the stage. In particular,

Table 1 Grid independence study.

Nodes /millions	Mass flow rate/(kg/s)	Total pressure ratio	Adiabatic efficiency
0.5	0.1724	2.1340	0.8308
1.0	0.1749	2.1453	0.8400
1.5	0.1769	2.1330	0.8448
2.0	0.1771	2.1365	0.8452

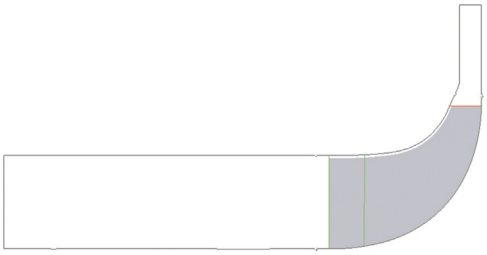

Figure 12 Meridional sketch for compressor stage.

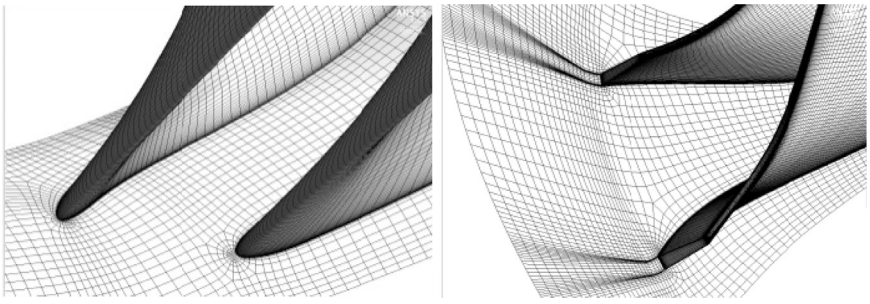

Figure 11 Grid topology.

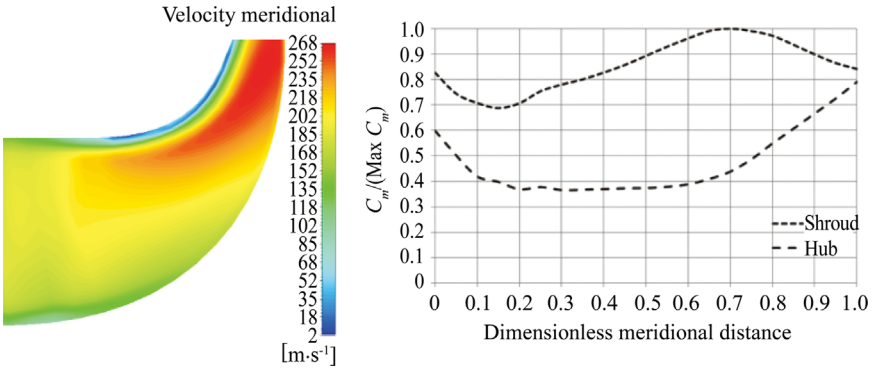

Figure 13 Meridional velocity (left) CFD, (right) preliminary design.

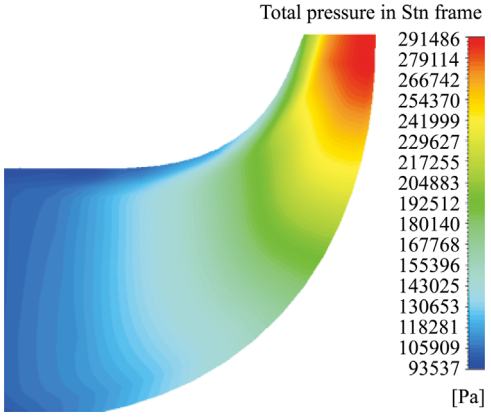

Figure 14 Total pressure contours.

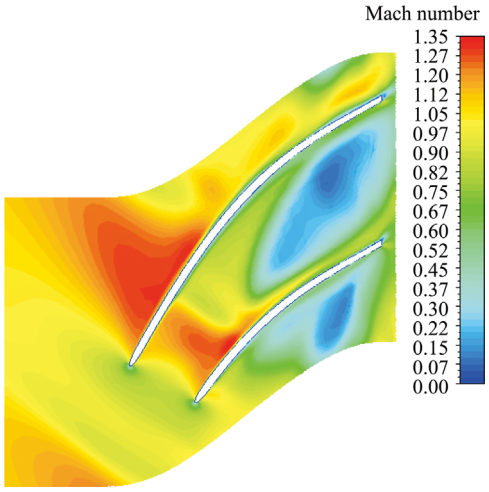

Figure 17 Mach number at 90% of span.

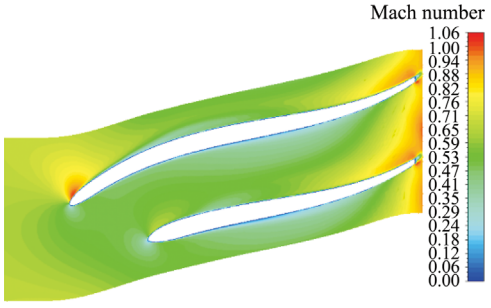

Figure 15 Mach number at 10% of span.

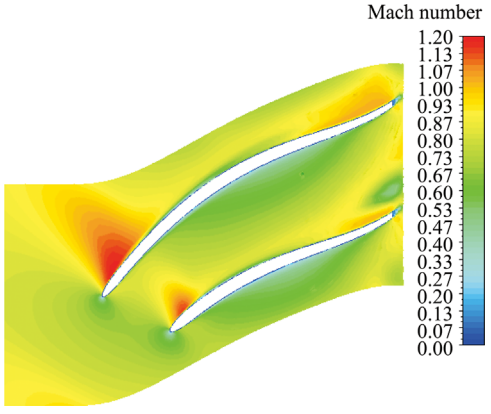

Figure 16 Mach number at 50% of span.

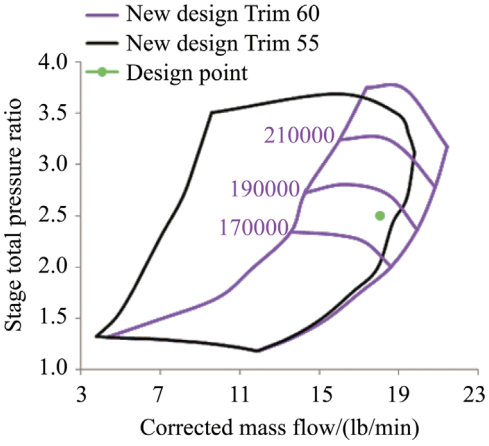

Figure 18 Trim 60 and Trim 55 compressor map comparison.

meridional velocity, absolute and relative Mach number and pressure distribution across a blade need to be checked at least at design condition to make sure that the flow behaves as expected. In the present study, these plots have been extracted at design condition for meridional velocity and total pressure on the meridional plot as shown in Figure 13 and Figure 14. The meridional velocity obtained through the CFD result is in good agreement with the preliminary

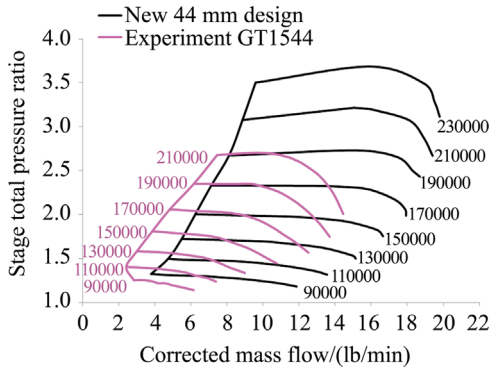

Figure 19 Total pressure ratio vs. mass flow rate.

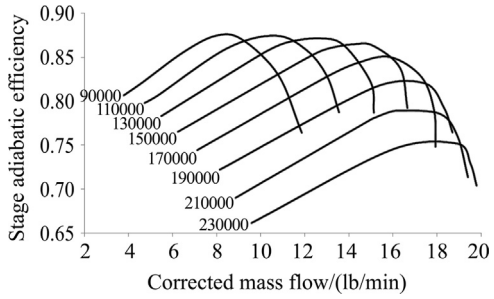

Figure 20 Adiabatic efficiency for Trim 55 impeller.

design meridional velocity trend. However, some disagreement at shroud region can be observed due to the tip clearance effect. Similarly, as expected, meridional velocity and total pressure increase from the inlet to outlet gradually. Losses are dominant in the blade tip region due to tip clearance flow which deteriorates the performance. Although these losses are unavoidable, an intensity of this loss can be minimized by keeping tip clearance value at a reasonable level [5,6,10,11].

Similarly, Mach number at 10%, 50%, and 90% spanwise locations have been shown on the blade to blade plot. Figure 15, Figure 16 and Figure 17 show an increasing trend of Mach number from hub to shroud region. As expected, the maximum relative Mach number appears at an inducer region. The distribution of these parameters is consistent with the general trend of flow behavior [12].

CFD simulations for eight-speed lines have been carried out to generate a full compressor map. The result shows a choke flow of 21.43 lb/min at 230 kRPM and peak efficiency around 87% at 110 kRPM. The CFD results also confirm that the design point attribute of 2.5 total pressure ratio and 18 lb/min mass flow rate at 185 kRPM has been achieved through this design. Even though a maximum mass flow and peak efficiency appear to be satisfactory, the surge boundaries are not up to the expectation. The poor map width is shown in Figure 18. This shortcoming could be vasued due to the limitation of numerical analysis which makes CFD simulations to diverge near stall boundaries.

To overcome this shortcoming, an inducer diameter of a blade is reduced from 60 trim to 55 trim. This leads to an improvement in surge margin at an expense of reduction in

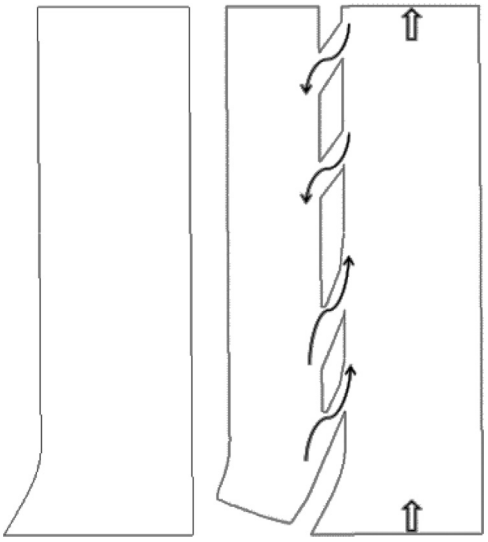

Figure 21 Standard diffuser (left) and enhanced diffuser (right).

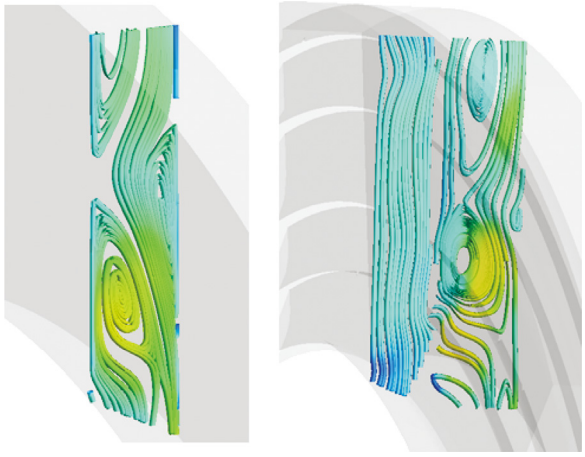

Figure 22 Flow vortices in diffuser.

choke flow. It is well understood that the mass flow rate through the compressor is proportional to the inlet diameter of the impeller and therefore reduction in trim or inducer diameter would certainly result in a reduction in mass flow [1,7]. Moreover, an improvement in surge margin can be attributed to the change in the blade angle at inducer region as the blade angle varies from hub to shroud at leading edge of the blade. Furthermore, trimming a blade shroud at the inlet, while keeping the blade exducer width unchanged can result in a change of slope in shroud contour which can be considered as the reason behind the extended surge margin for lower trim configuration. The obtained result for Trim 55 compressor wheel is shown in Figure 18, depicting a total pressure ratio against mass flow rate. The result shows a significant improvement in surge margin with around 87% peak efficiency. The efficiency curves for different rotational speed are shown in Figure 20. The comparison of these speed lines with experimental data of Garrett turbocharger GT1544 has been done in order to verify the outcomes of the present design. GT1544 configuration has

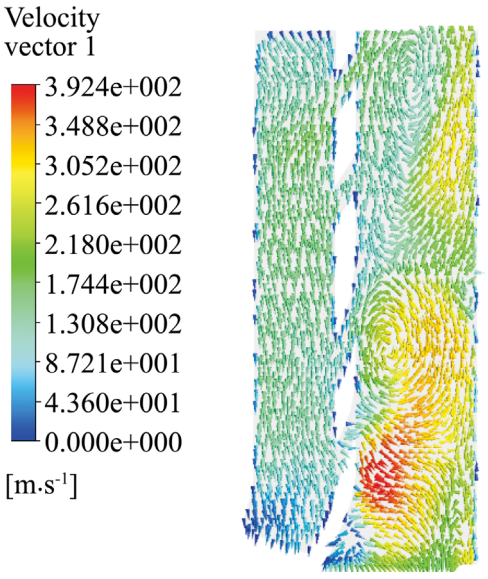

Figure 23 Velocity vector in an enhanced diffuser.

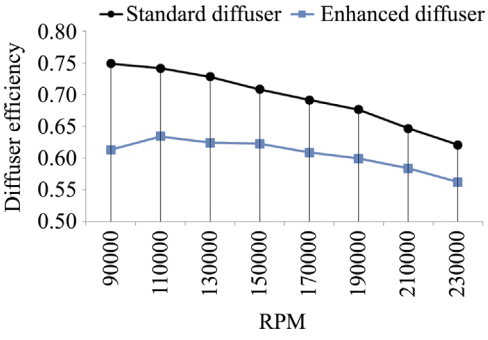

Figure 24 Diffuser efficiency.

43.9 mm diameter compressor wheel with 56 trim and suitable for comparison due to same wheel diameter dimensions. As shown in Figure 19, the present design have 34% improvement in choke flow at 210 kRPM. As CFD simulations are carried out without volute geometry due to the limitation of computational capability, the performance in terms of total pressure ratio and adiabatic efficiency appears to be over-predicted. The peak efficiency of the stage in CFD simulation appears to be around 87%. However, after incorporation of volute, a rough estimation of stage efficiency can be about 81% with 6% of loss in efficiency since volute introduces severe loss in total pressure and bring stage total pressure ratio and efficiency at a lower level [13,14]. This performance estimate would be confirmed on completion of full stage gas stand test.

Additionally, surge margin achieved through this design looks smaller compared to GT1544 surge margin. Therefore, an improvement in surge margin needs to be addressed for the current design. One option is to further reduce a trim of a blade which shift entire map towards left by a certain percentage and improve surge margin which could match to GT1544 surge line but at a cost of reduction in choke flow [14–16].

In order to keep choke flow intact and to improve surge margin, a new surge margin improvement technique is proposed. This technique mainly concentrates on diffuser enhancement in which a flow inside the diffuser is recirculated through supplementary diffuser cavity as shown in Figure 21.

In context of enhanced diffuser, as a reverse flow occurs into a main diffuser passage, the flow passes through top two cavity channels and enters the cavity, the bottom two channels collect the flow from the cavity and release it into the main diffuser passage. This technique results in delaying stall and improves surge margin. To validate this flow mechanism, CFD simulations have been carried out with standard and enhanced diffuser stage. As shown in Figure 22, the flow in diffuser appears to be very complex with severe separation eddies, particularly at stall region.

This sort of flow behavior causes compressor stage to surge due to blockage and reversing of flow, hence, the addition of such cavity would lead to recirculate the flow near diffuser shroud region, making compressor stage to sustain longer in operation.

The flow mechanism across a recirculation cavity and diffuser can be further illustrated in a flow vector plot as shown in Figure 23. Effectively, this flow mechanism reduces the flow blockage by allowing separated flow to enter the cavity through top channels and energized the main stream flow by discharging air from the cavity into it, which ultimately results in providing an additional momentum to air flow, particularly in stall operating conditions.

Ideally, the top two cavity channels are used to collect air and recirculate it into the main stream through bottom two channels. However, due to the complexity and random nature of the flow, it should be noted that the flow can travel in either direction depending on the pressure difference across the cavity and diffuser flow.

Moreover, the structure of such cavity also plays a vital role in the effectiveness of recirculation mechanism. Therefore, care must be taken to exploit the available space rationally in the vicinity of diffuser while keeping the packaging constraints into mind. However, as design guideline, it is recommended that the slope of cavity channel should be kept at around 30° or less measured with respect to the vertical direction with cavity width around 1 mm. This would facilitate smooth flow into the cavity through top channels. Additionally, care also must be taken to position the bottom flow-out channel as steep as possible to discharge the flow tangential to diffuser main stream flow. This is necessary in order to mix cavity flow with diffuser mainstream flow without disturbing its main flow path. In the current case, four cavity channels are used for larger recirculation of flow; however, this number can be varied depending upon the availability of radial space or the height of diffuser.

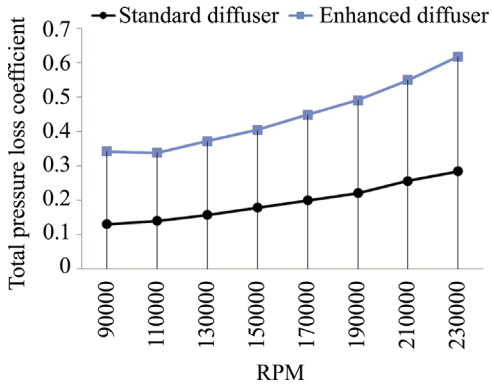

Figure 25 Diffuser total pressure loss coefficient.

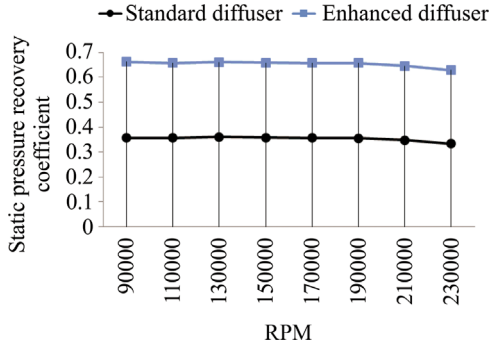

Figure 26 Diffuser static pressure recovery factor.

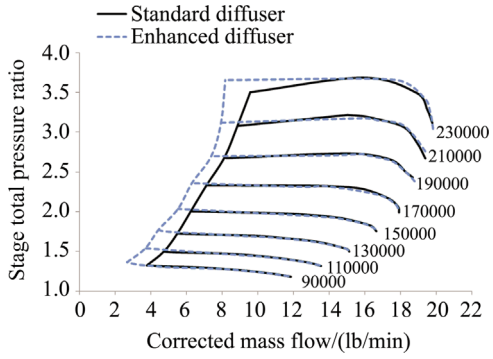

Figure 27 Total pressure ratio for standard and enhanced diffuser.

It is inevitable to have more losses in an enhanced diffuser as compared to the standard diffuser. As the primary objective of this mechanism is to improve the surge margin, therefore, compromise in diffuser performance is necessary. Ideally, diffuser performance can be evaluated by means of diffuser efficiency, total pressure loss coefficient and static pressure recovery coefficient [3]. These parameters have been computed using Eqs. (7)–(9) respectively, and comparison of theses parameters have been made along the surge line for standard and enhanced diffuser cases.

$$\eta_D = \frac{\left(P_3/P_2\right)^{(\gamma-1)/\gamma}-1}{\left[\left(P_{02}/P_{03}\right)\left(P_3/P_2\right)\right]^{(\gamma-1)/\gamma}-1} \tag{7}$$

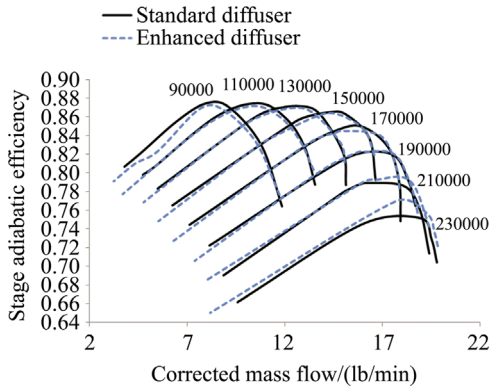

Figure 28 Stage efficiency for standard and enhanced diffuser.

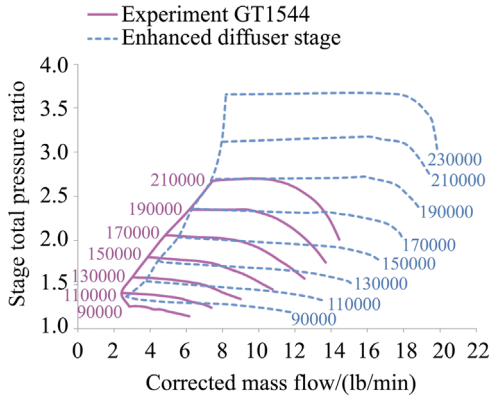

Figure 29 Comparison of GT1544 and enhanced diffuser stage.

$$\overline{\omega} = \frac{P_{02}-P_{03}}{P_{02}-P_2} \tag{8}$$

$$C_p = \frac{P_3-P_2}{P_{02}-P_2} \tag{9}$$

In fact, it can be observed that an overall diffuser performance has been deteriorated due to highly complex flow in an enhanced diffuser. It would be difficult to compare the performance of both diffusers at a same operating point in the map, however, an attempt has been made to compare performance along the respective surge line. As shown in Figures 24–26, on average, an enhanced diffuser produce 12% decrease in diffuser efficiency, 31% increase in total pressure loss coefficient and 15% decrease in static pressure recovery coefficient along the surge line. Therefore, it is worthwhile, to optimize the overall structure of the design to improve the performance of diffuser while keeping the surge margin improvement as the primary objective.

The performance map achieved through this technique is compared with the stage result having standard diffuser geometry in Figure 27 and Figure 28. As per simulation results, on average 16% of surge margin improvement has been achieved as compared to standard diffuser stage. The stage efficiencies more or less remain the same in both

cases, however, around 1% of peak efficiency advantage has been observed at the maximum speed line in enhanced diffuser stage case.

Furthermore, as shown in Figure 29, a comparison plot between GT1544 experimental data and enhanced diffuser stage still shows a shortage of surge margin, particularly at low RPM region. This shortcoming will be addressed by means of further optimizing an enhanced diffuser geometry and diffuser width. Due to the limitation of computational capability, volute has not been included in compressor stage. Attempts well be made to carry out a full stage simulations with the inclusion of volute geometry in a high capacity computer cluster.

8. Conclusions

A new approach in centrifugal compressor design has been carried out with 44 mm exducer diameter and Trim 60 for vaneless diffuser stage configuration. This design is intended to achieve improved performance as compared to existing 44 diameter aftermarket wheel families. CFD approach has been utilized to assess aerodynamic performance of the stage. As a results, a new compressor stage with Trim 60 provides a choke flow of 21.43 lb/min at 230000 RPM and peak efficiency of 87% at 110 kRPM, while satisfying the design point attribute of 2.5 total pressure ratio and 18 lb/min mass flow rate at 185 kRPM, but surge margin appears to be insufficient. Hence, compressor trim has been reduced to Trim 55 to improve the surge margin. The CFD result obtained for this configuration shows a 34% increase in choke flow compared to GT1544 experimental data at 210 kRPM. Furthermore, a new approach to improve surge margin by means of diffuser enhancement is proposed. This approach provides an average of 16% increase in surge margin compared to standard diffuser stage without altering choke flow and stage efficiencies. Assessment of structural integrity of compressor wheel with aluminum alloy 2014-T6 has been carried out. The modal analysis shows the first mode shape of frequency at blade inducer. Likewise, the maximum equivalent (von-mises) stress 330 MPa appears in compressor bore region with stress magnitude well below the yield strength 345 MPa of the material.

Acknowledgment

The research was jointly supported by European Horizon 2020 grant 644971 and Innovate UK grant 104021. The Authors wish to thank Birmingham High Performance Turbomachinery and Advanced Design Technology Limited for their support.

References

[1] M. Casey, D. Rusch, The design space boundaries for high flow capacity centrifugal compressors, in: Proceedings of ASME Turbo Expo, Copenhagen, Denmark, 2012.
[2] S.Y. Cho, K.Y. Ahn, Y.D. Lee, Y.C. Kim, Optimal design of a centrifugal compressor impeller using evolutionary algorithms, Math. Probl. Eng. 2012 (2012) 22 no. 0.1155/2012/752931.
[3] R.H. Aungier, Centrifugal Compressor: A Strategy for Aerodynamic Design and Analysis, ASME Press, New York, 2000.
[4] P. Roytta, A. Gronman, A. Jaatinen, J. Backman, T.T. Saaresti, Effects of different blade angle distributions on centrifugal compressor performance, Int. J. Rotating Mach. 2009 (2009) Article ID 537802.
[5] A.H. Zahed, N.N. Bayomi, Design procedure of centrifugal compressors, ISESCO J. Sci. Technol. 10 (17) (2014) 77–91.
[6] M.P. Boyce, Principles of operation and performance estimation of centrifugal compressors, in: Proceedings of the Twenty-Second Turbomacjinery Symposium, 1993.
[7] C. Xu, R.S. Amano, Meridional considerations of the centrifugal compressor development, Int. J. Rotat. Mach. 2012 (2012) Article ID 518381.
[8] M. Zangeneh, A. Goto, H. Harada, On the role of three-dimensional inverse design methods in turbomachinery shape optimization, in: Proceeding of Institute of Mechanical Engineering, Vol. 213, Part C, 1999.
[9] C. Xu, R.S. Amano, Empirical design considerations for industrial centrifugal compressors, Int. J. Rotating Mach. 2012 (2012) no. 10.1155/2012/184061.
[10] M. Casey, D. Krahenbuhl, C. Zwyssig, The design of ultra-high-speed miniature centrifugal compressors, in: Proceedings of European Conference on Turbomachinery Fluid Dynamics and Thermodynamics, ETC 10, Zurich, Switzerland, 2013.
[11] C. Gu, Y. Song, P. Li, A new optimization method for centrifugal compressors based on 1D calculations and analyses, Energies 8 (2015) 4317–4334 no. 10.3390/en8054317.
[12] H. Tamaki, M. Unno, T. Kawakubo, Y. Hirata, Aerodynamic design of centrifugal compressor for AT14 Turbocharger, IHI Eng. Rev. 43 (2) (2010).
[13] X.Q. Zheng, J. Huenteler, M.Y. Yang, Y.J. Zhang, T. Bamba, Influence of the volute on the flow in a centrifugal compressor of a high-pressure ratio turbocharger, Proc. IMechE: J. Power Energy 224 (2010).
[14] R. Pauer, N. Muller, Impeller design for radial and mixed flow compressors, in: 2004 ASME International Mechanical Engineering, Anaheim, California USA, 2004.
[15] C. Roger, The efficiencies of single-stage centrifugal compressors for aircraft applications, in: International Gas Turbine and Aeroengine Congress and Exposition, Orlando, FL, 1991.
[16] Garrett Turbochargers, URL: ⟨https://turbobygarrett.com/turbobygarrett/turbochargers⟩.